 https://doi.org/10.3311/PPee.36872

Periodica Polytechnica Electrical Engineering and Computer Science, 69(3), pp. 268–279, 2025

Modeling and Performance Analysis of 3D Structured Rectilinear Rogowski Coil Using Finite Element Method

Priti Bawankule[1], Kandasamy Chandrasekaran[1*]

[1] Department of Electrical Engineering, National Institute of Technology Raipur, G.E. Road, 492010 Raipur, Chhattisgarh, India
[*] Corresponding author, e-mail: kchandrasekaran.ee@nitrr.ac.in

Received: 13 March 2024, Accepted: 26 May 2025, Published online: 13 June 2025

Abstract

This paper proposed a discrete Rogowski coil (RC) model, consist of rectilinear solenoids (*S*) connected in series. This model is designed using ANSYS Maxwell software for different shape of primary conductor and the mutual inductance (*M*) between RC model are calculated. The paper discussed about impact of various shape and different position of primary conductor. The *M* between the RC model and straight circular, rectangular cross section and D-shaped conductors are evaluated using the Finite Element Method (FEM). The effect of cross section of primary conductor on *M* has analyzed and reported. For larger numbers of *S*, eccentricity of conductor will decrease so that output of coil is also improved. In this study, the distribution of magnetic field is examined for changes in the position of the conductors. The designed RC model output is studied with respect to the power and high frequency input signals. A discrete RC is tested using simulated standard sinusoidal and impulse (8/20 μs) as an input signal. Performance of the RC is analyzed, and its results for the different input magnitude is reported. An output characteristic and sensitivity of the designed RC have also been determined and reported.

Keywords

eccentricity error, Finite Element Method, mutual inductance, Rogowski coil, sinusoidal current, impulse current

1 Introduction

Rogowski coil (RC) is a device that, measures alternating and transient current. Due to saturation problems in magnetic cores, conventional electromagnetic current sensors are unable to accurately measure high ampere currents [1, 2] whereas the RC works differently: its skeleton is made of non-ferromagnetic materials, and its turns are evenly wound. In several industries, the RC is widely used because of its simplicity, minimum cost, manageable weight, linear, dynamical, non-invasive, and immune to saturation of the core [3–7]. As RC is wrapped around current carrying conductors, they generate inductive voltages. Mutual inductance (*M*) is an important constraint amongst the inductive voltage and the primary conductor. To improve RC accuracy, it is important to investigate the influence of quantities on *M* [8–11].

Xu et al. [4] described the discrete RCs, known for their flexible structure and scalability in production. Employing the magnetic vector potential (MVP) approach, it calculated *M* between discrete RCs and circular and rectangular primary conductors, corroborated the method's simplicity compared to the Finite Element Method (FEM). The analysis investigates how parameters such as conductor inclination, cross-section, and eccentricity affect the accurateness of RC measurements, identifying optimal solenoid (*S*) characteristics, also in that paper experimental validation of a discrete RC prototype aligns closely with calculated values, while assessments reveal reduced interference from external currents with increased separation distance.

Liu et al. [8] described on-site measurements, RCs exhibit diverse shapes, posing challenges for accurately calculating their electrical properties, especially those with curved skeletons and circular cross-sections. Liu et al. [8] addressed challenges in theoretical framework for computing *M* between primary conductors of different shape and RCs with different cross-section, also this study explores the impact of various skeleton shapes of RCs and primary conductor configurations on *M*, comparing ideal scenarios with non-ideal ones. Based on literature survey, it is observed that reveal crucial insights to enhance measurement accuracy: circular skeleton deformations should be minimized,

Cite this article as: "Modeling and Performance Analysis of 3D Structured Rectilinear Rogowski Coil Using Finite Element Method", Periodica Polytechnica Electrical Engineering and Computer Science, 69(3), pp. 268–279, 2025. https://doi.org/10.3311/PPee.36872

coils with curved angles are preferable, primary conductors should maintain straightness and pass across the center of coil. Additionally, for RC with rectangular skeletons, a novel structure is proposed to mitigate deviation effects induced by the primary conductor. Liu et al. [9] discussed the comparison of traditional toroidal RCs with rectilinear *S* offer easier and more cost-effective realization. Therefore, exploring the effectiveness of discrete RCs becomes significant. This literature paper studied and employs a MVP formulation to numerically analyzed the electromagnetic and geometrical properties of discrete RCs also investigated the ability of different configurations to resist external magnetic fields. In Marracci et al. [10], Ferković et al. [11] and Ferković et al. [12], a study of the crucial factors that influence the *M* of RC and a straight primary conductor is presented. In the study primary conductors of the sensors are straight and placed in the coil hole, while the skeleton has circular, and the cross-section has rectangular. Recent innovations in RC design have been achieved using printed circuit board technology. It is difficult to minimize the size of inductance coil sensors because their sensitivity depends on their core length as per literature survey.

Chen et al. [13], Wang et al. [14] and Liu et al. [15] discussed M of the PCB based RC can be measured under conditions that includes eccentricity, external parallelism, and perpendicular of the primary conductor. The discussion revolves around the development of micro coil sensors, featuring dimensions less than 1 mm.

The discrete RC model has several advantages over traditional toroidal coils, particularly in industrial applications requiring compact and lightweight designs [16]. Unlike loop coils, which face challenges in miniaturization, mass production, and cost-effectiveness, discrete RCs are easier and more affordable to manufacture due to their rectilinear *S* structure. This design simplifies fabrication, reduces production complexity, and enables efficient large-scale manufacturing. Additionally, discrete RCs are easier to install, making them a practical choice for current measurement in power systems, including circuit breakers. Their ability to measure high-frequency and high-magnitude currents provides enhanced performance while maintaining a smaller footprint. Combining these factors makes the discrete RC model a highly reliable and cost-effective solution for industrial current measurement applications. Thus, it is important to investigate the performance of a discrete RC.

Halim et al. [17] and Istrate et al. [18] discussed the creation of an impulse current generator with an 8/20 μs waveform, vital for testing surge arresters used in lightning protection. As direct lightning testing isn't feasible, the generator is developed, with precise circuit component calculations and computer simulations to ensure accuracy. A scaled-down experimental setup mimics natural lightning patterns, assessing the generator's ability to test arrester blocks up to 100 kV and 4 kA ratings. Metwally [19, 20] introduced a self-integrating RC for high-impulse current measurement, analyzing its performance and design principles. Measurement tests demonstrated the coil's linearity and accuracy in capturing impulse current waveforms, including overdamped scenarios. To enable voltage integration without relying on external circuitry, the lumped parameter model of an RC circuit was studied in Istrate et al. [18]. Furthermore, sinusoidal current measurements were conducted using a RC for various values of terminal resistance [21]. Dubickas and Edin [22] analyzed the high frequency of model of RC with small number. RC eccentricity [23] and tied with bar conductor [24] analyzed using FEM approaches. Magnetic shield model [25], improved magnetic shield model [26] of RC investigated. The analysis focuses on the rectangular cross-section of a RC with varying arrangements of turns, specifically considering non-circular coil configurations investigated in Fu et al. [27].

Numerous researchers predominantly focus on numerical, theoretical and experimental approach for analyzing RC. However, limited research has been conducted on the design and modelling of RCs in a 3D structure in ANSYS Maxwell [28] using the FEM. This paper focuses on design and modelling of a 3D structure of discrete RC in ANSYS Maxwell [28].

The primary aims of this paper can be outlined as follows:

- The new proposed 3D structured rectilinear RC model, designed in ANSYS Maxwell software [28], and analyzed using FEM.
- This investigation focuses on calculating *M* for various primary conductor shapes, including straight rectangular, straight circular, and D-shaped, using FEM. Additionally, the effect of rectangular conductor dimensions on the *M* of the RC model is analyzed.
- The influences of position of conductor and increasing the number of *S* on the measurement accurateness of RC model is analyzed and eccentricity of coil evaluated and reported.
- The impact of different input signals on designed RC output are investigated. Performance of RC is tested with two signals such as high amplitude sinusoidal

power frequency and high amplitude impulse current (8/20 μs).

The paper is structured as follows: Section 2 elaborates on the rectilinear 3D structure of the RC and discusses the *M* of the model. Section 2 analyzed the effect of different shape and dimension of primary conductor of *M* of RC. In Section 3, the investigation focuses on assessing the effects of the primary conductor's position, increasing the number of *S* on the measurement accuracy of the RC model, and evaluating the eccentricity of the coil. Section 4 presenting the result for the testing RC model for two different signals high amplitude sinusoidal power frequency and high amplitude impulse current (8/20 μs). Lastly Section 5 concludes the paper by summarizing main key points of results.

2 Mutual inductance of proposed RC model

The RC, an electromagnetic sensor, operates on Faraday's law, measuring AC currents through electromagnetic induction. Its flexible coil wound around a non-magnetic core detects changes in the magnetic field generated by the current-carrying conductor. Widely utilized in power systems monitoring and electrical safety testing, the RC offers precise measurements with its broad bandwidth and high accuracy, correlating induced electromotive force (EMF) in the loop with the time-varying magnetic flux (Φ) according to Faraday's law.

The 3D model of RC is designed in ANSYS Maxwell software [28] for calculating the *M* of model. A proposed RC model consists of four rectilinear *S* connected in series as shown in Fig. 1. The model of circular cross-section of primary conductor and one *S* coils as shown in Fig. 2.

The total mutual inductance of the RC model is denoted by *M*. The *M* between each rectilinear *S* and conductor is M_i. In RC model, total *M* is the sum of the *M* of each *S* as given in Eq. (1):

$$M = \sum_{i=1}^{4} M_i. \tag{1}$$

The output of RC in terms of mutual inductance [28] is given in Eq. (2):

$$v(t) = -M\frac{di(t)}{dt}, \tag{2}$$

where $i(t)$ and $v(t)$ are instantaneous value of primary current and induced voltage of RC model, respectively.

The change in cross-section dimensions of primary conductor is effects performance of RC. Hence, straight circular, rectangular cross-section and D-shaped primary

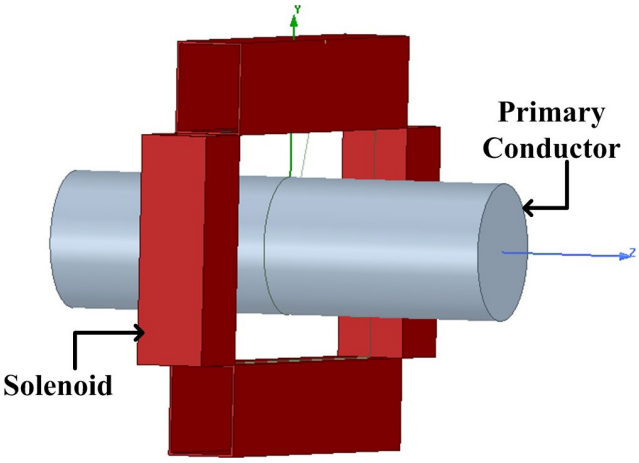

Fig. 1 3D RC model with four rectilinear *S*

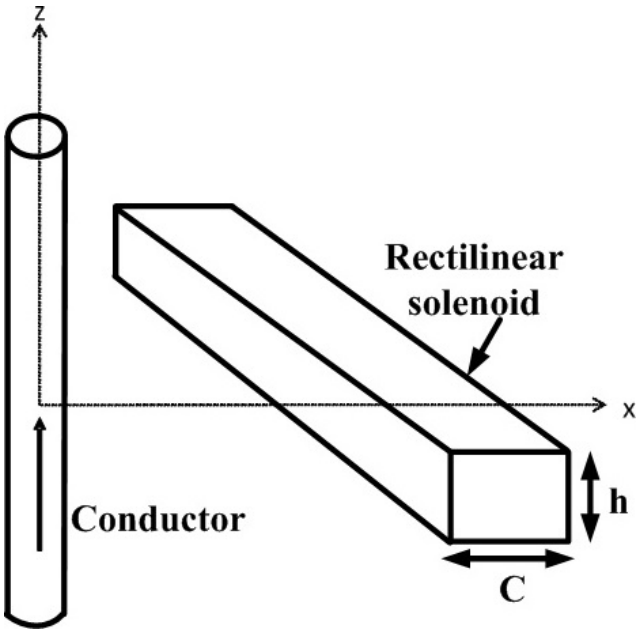

Fig. 2 Model of rectilinear *S* and primary conductor

conductor with air core are considered for calculating the *M* of designed RC model. In addition, the primary conductor position is also giving a considerable impact on *M* that effect on measurement accuracy. As the conductor is placed at off center of coil, eccentricity error (*E*) will be there, and it is calculated as given in Eq. (3):

$$\text{Eccenticity error}(E) = \frac{|M_p - M_o|}{M_o} \times 100\%, \tag{3}$$

where M_p indicated the *M* when primary conductor placed at off center of coil and M_o represent the *M* when the primary conductor is placed at the center.

Bawankule and Chandrasekaran [29, 30] discusses the design of the RC and analyses *M* through FEM.

2.1 Effect of straight circular, rectangular cross-section and D-shaped primary conductor on *M*

The model one rectilinear *S* and primary conductor as presented in Fig. 2. The performance of RC is analyzed with different structure of primary conductors as shown in Fig. 3 to Fig. 5. The straight circular cross-section conductor with 1 mm radius is located at center and off center of RC is shown in Fig. 3 (a) and (b). Similarly, straight rectangular cross-section with a = 6 mm, b = 3 mm and D-shaped circular cross-section with 1 mm radius is placed at center and off center of RC is shown in Fig. 4 (a) and (b), and Fig. 5 (a) and (b), respectively. The number of turns for the *S* RC_1 and RC_3 is 500, and for RC_2 and RC_4 is 1000. The RC model has width and height is C and h, respectively (i.e., $C \times h = 4 \times 3$ mm) presented in Fig. 2. The coil is made of copper material and conductor is aluminum.

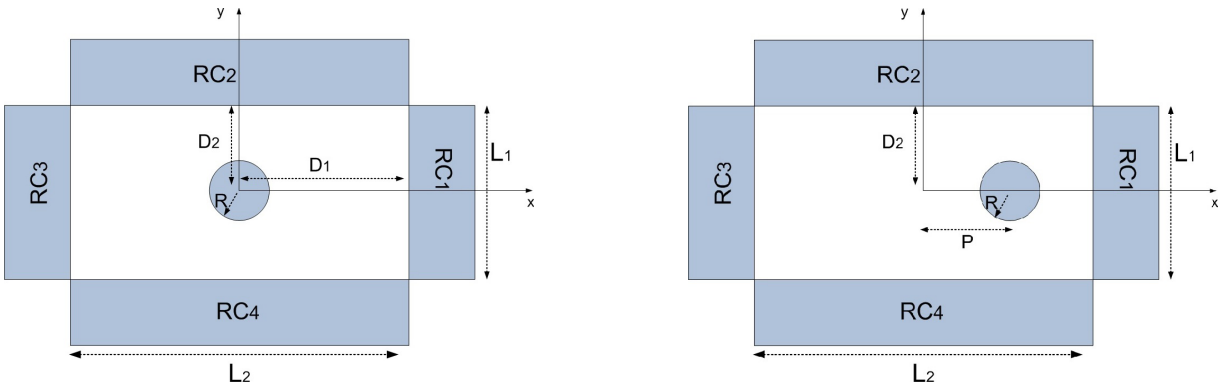

(a) (b)

Fig. 3 Circular conductor with R = 1 mm, h = 3 mm, L_1 = 10 mm, L_2 = 10 mm, D_1 = 10 mm, D_2 = 5 mm: (a) at center; (b) at off-center (P = 5 mm) of RC model

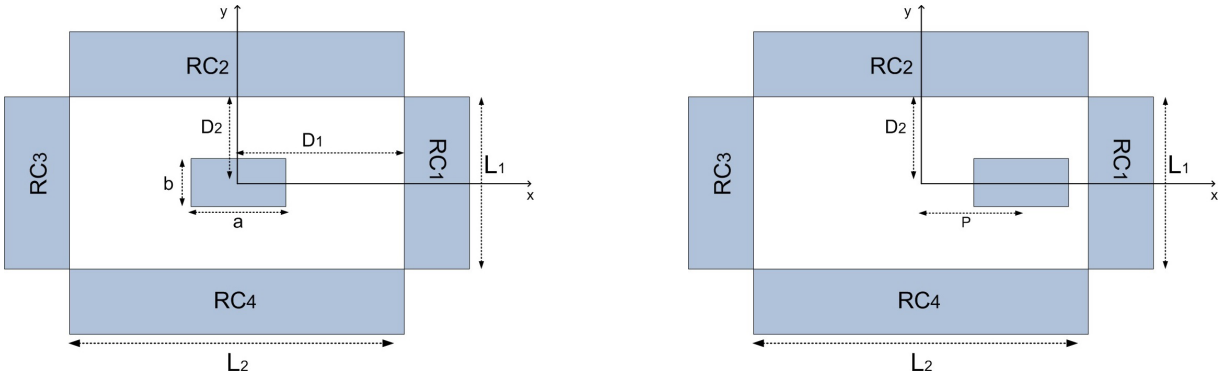

(a) (b)

Fig. 4 Rectangular conductor with a = 6 mm, b = 3 mm, L_1 = 10 mm, L_2 = 10 mm, D_1 = 10 mm, D_2 = 5 mm: (a) at center; (b) at off-center (P = 5 mm) of RC model

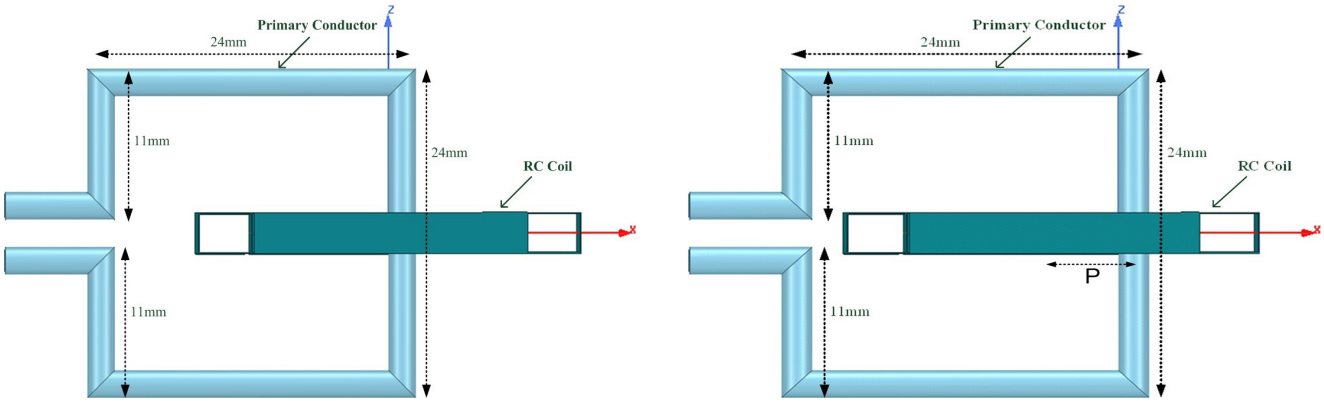

(a) (b)

Fig. 5 D-shaped primary conductor: (a) at center; (b) at off-center (P = 5 mm) of RC model

The primary conductor off center position is at a distance '*P*' from center towards the x-axis. It will affect the *M* of the RC model and also the accuracy of the measurement; hence it is important to calculate eccentric error of coil.

The impact of shape of primary conductor on *M* of coil is tested with the input of 400 A sinusoidal current with the frequency of 50 Hz. The *M* between the primary conductor and each rectilinear *S* RC_1, RC_2, RC_3 and RC_4 is calculated and its results are presented in Table 1. The simulation result shows that the straight circular conductor and D-shaped conductor with the same radius gives different *M*. It is 661.1881 nH for circular conductor and 663.7876 nH for D-shaped conductor with respect to centre of RC.

The performance of RC is analyzed with different structure of primary conductors as shown in Fig. 3 to Fig. 5. The straight circular cross-section conductor with 1 mm radius is located at center and off center of RC is shown in Fig. 3 (a) and (b) respectively. Similarly, straight rectangular cross-section with a = 6 mm, b = 3 mm and D-shaped circular cross-section with 1 mm radius is placed at center and off center of RC has been illustrated in Fig. 4 (a) and (b), and Fig. 5 (a) and (b), respectively. The number of turns for the *S* RC_1 and RC_3 is 500, and for RC_2 and RC_4 is 1000. The RC model has width and height is *C* and *h*, respectively (i.e., $C \times h = 4 \times 3$ mm).

From Table 1, it is clear that for circular and rectangular conductor positioned at center, *M* of RC_1 and RC_3 are nearly equal. Similarly, RC_2 and RC_4 *M* is close to each. For off center position, *M* of coil *S* close to primary conductor is more. In order to obtain better output accuracy, eccentric error needs to calculate for different position of the conductor. From simulation result it is seen that, *E* for circular, rectangular and D-shaped are 2.229%. 0.024822% and 0.5533% respectively. In case of circular cross-section, there is much difference in *M* observed between conductor placed at center and off-center. Therefore, *E* is more for conductor with circular cross-section.

2.2 Main effect of dimension of rectangular primary conductor on *M* of RC model

The parameters of rectangular cross-section '*b*' and '*a*' (width and length) affect *M* of coil as given in Fig. 3. Here '*b*' is fixed to 3 mm and '*a*' is altered from 3 to 14 mm then, the change of *M* of RC model is simulated, and its results are plotted in Fig. 6. From Fig. 6, it is seen that, the *M* is decrease from 665.06 to 651.556 nH for increasing length of rectangular cross-section conductor.

3 Effect of number of *S* and position of primary conductor on *M*

Section 3 discussed about the effect of number of *S* on *E*. It is possible to make a RC model more analogous to conventional circular RC by increasing the number of *S* [4]. As imaginable cases, when number of $S \rightarrow \infty$, the RC model can appear as a circular RC, then Ampere's law will fully apply, and the *E*s of the discrete coil will move towards zero. But practically it is not possible that $S \rightarrow \infty$. For simulation purpose number of *S* considered under study are *S* = 4, 6 and 8 and the same is designed and shown in Fig. 7. The length of all *S* within the model is same, which is taken as 10 mm, and the cross-sectional radius of primary conductor is 1 mm. These *S* arranged in inscribe circle with 500 turns on each *S*, also $C \times h = 4 \times 3$ mm.

The primary conductor is placed at different position from I_1 to I_{11} with reference to the RC model shown in Fig. 8. The calculation of the eccentric error has been conducted for three different scenarios, corresponding to the positions of the primary conductor, specifically when *S* = 4, *S* = 6, and *S* = 8.

Results of *M* of RC models with *S* = 4, 6 and 8 as shown in Fig. 7 at various positions I_1 to I_{11} of the primary conductor is given in Table 2. From simulation result it is observed that, for *S* = 4, the *M* is in the range of 589.41 to 615.46 nH, for *S* = 6, the range is from 596.91 to 601.11 nH, also for *S* = 8, the range is from 608.78 to 609.34 nH. In case of

Table 1 *M* of RC model with different cross-sections of primary conductor

Cross-section	Position	*M* (nH)				
		RC_1	RC_2	RC_3	RC*4*	RC model
Circular	Center	64.9977	265.5258	64.8779	265.7865	661.1879
	Off-center	158.0101	230.9990	26.1002	231.3393	646.4486
Rectangular	Center	62.1412	265.0698	63.6519	273.3349	664.1978
	Off-center	162.1208	227.7896	26.4686	231.7313	648.1103
D-shaped	Center	59.4135	242.0353	120.5490	241.7902	663.788
	Off-center	145.2658	178.5305	165.3043	178.3604	667.461

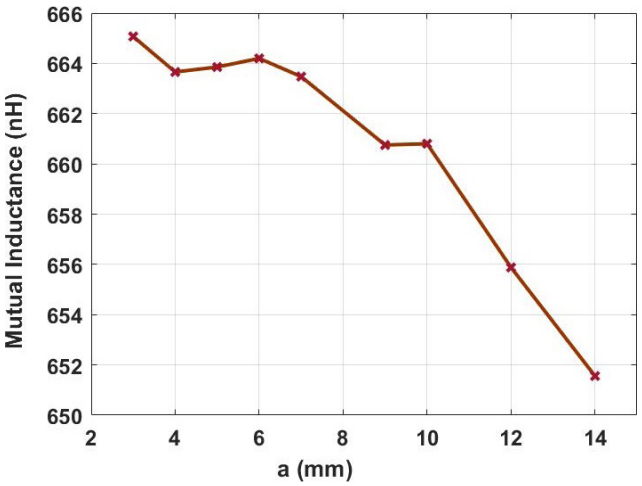

Fig. 6 Impact of length of rectangular conductor on *M*

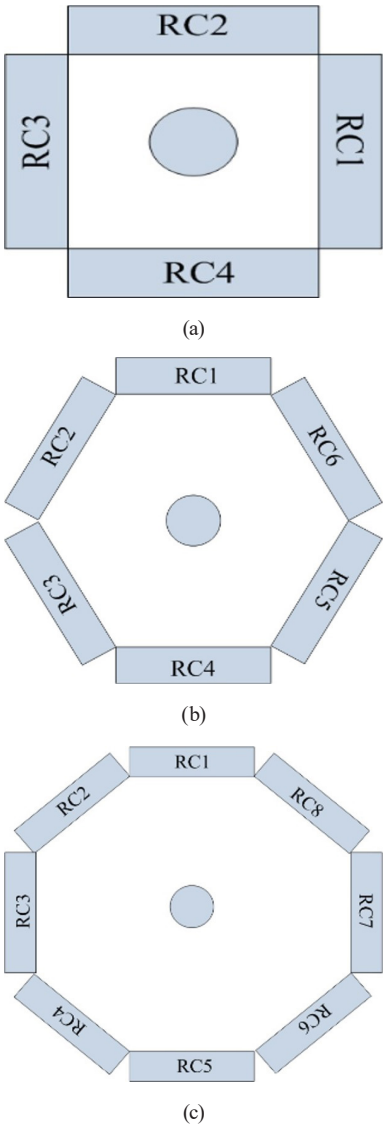

Fig. 7 RC model with different number of *S*: (a) *S* = 4; (b) *S* = 6; (c) *S* = 8

S = 4, the *M*, fluctuates more when the location of primary conductor is different position, results are compared for

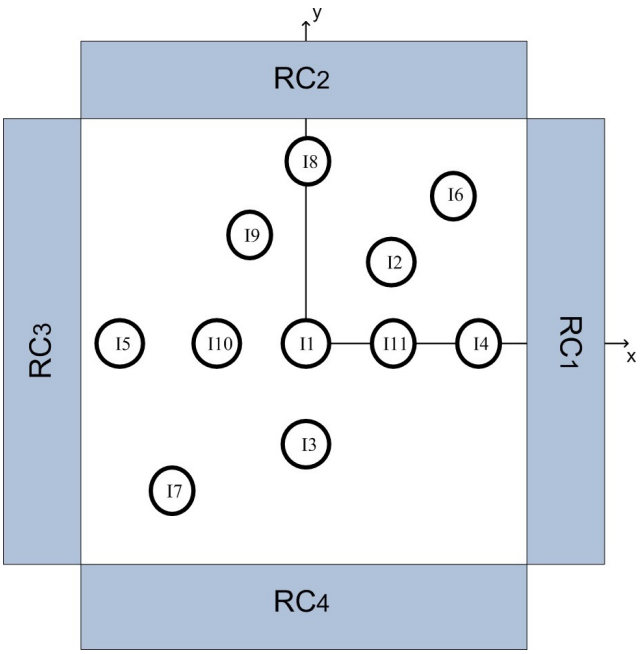

Fig. 8 Different position of primary conductor for *S* = 4 RC model

Table 2 *M* of RC model for different position of primary conductor

Position	*x* (mm)	*y* (mm)	*M* of RC model (nH)		
			S = 4	*S* = 6	*S* = 8
I_1	0	0	607.87	598.83	609.01
I_2	2	2	607.77	599.01	609.08
I_3	0	−3	610.12	600.27	609.24
I_4	3.8	0	614.07	596.98	609.34
I_5	−3.8	0	615.46	596.91	609.16
I_6	3.6	3.6	589.41	598.82	608.78
I_7	−3.6	−3.6	589.55	598.78	609.24
I_8	0	3.8	613.69	601.11	609.23
I_9	−2	2.5	606.55	599.18	609.19
I_{10}	−3.2	0	612.64	597.68	609.18
I_{11}	3.2	0	612.07	597.38	609.18

S = 6 and *S* = 8. For *S* = 8, there is minimal fluctuation in *M* when location of conductor changes.

Primary conductor closer to corner of RC model has lower *M* than conductor farther from corner. For *S* = 4 and *S* = 8, the position I_4 and I_5 close to the *S* have the highest *M*. Similarly for *S* = 6, the position I_8 near the *S* has the highest *M*. The *E* for the different positions of conductor for *S* = 4, 6 and 8 are illustrated in Fig. 9.

From the Fig. 8, it is seen that, highest *E* is occurring for *S* = 4 at I_6 position compared to *S* = 6 and 8 and it is 3.0357%. For *S* = 6 the maximum eccentric error is 0.3807% at I_8 position and for *S* = 8, it is 0.053% at I_4 position. From these results, it is clear that the *E* decrease for increasing the number of *S*.

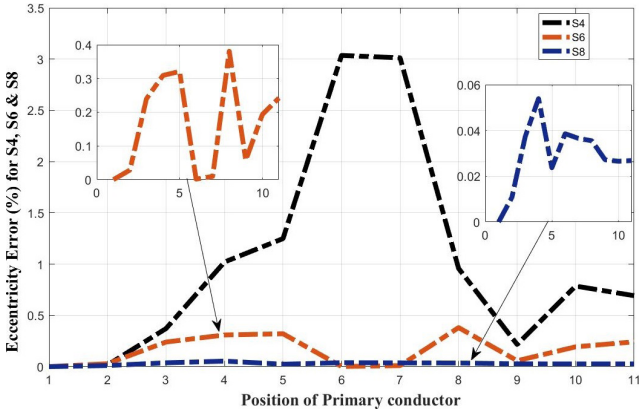

Fig. 9 E for the different positions of primary conductor

In this paper effect of off-center placement of a conductor on magnetic fields of RC model is also investigated, considering the position at I_4. The magnetic field vector result obtained for conductor placed at center and off-center for designed RC model with S = 4, 6 and 8 by using FEM is shown in Figs. 10 to Fig. 12, respectively. Simulation result shows that, magnetic field is maximum near the conductor, and it is decreases as the distance between the conductor and RC is increases.

The magnetic field concentration is uniform for conductor placed at center in all RC, but when conductor is placed at the I_4 position, the magnetic field concentration is non uniform. For S = 4, 6 and 8 as long as the conductor is placed at center of coil, the magnetic flux links are uniform across RC_1, RC_2, RC_3 and RC_4. However, when the conductor is placed off center i.e., at position I_4, for S = 4, the magnetic flux links with RC_1 are more than those with RC_2 and RC_4. For S = 8, flux links with RC_7 are more than those with other RCs. But for S = 6, there is no such variation observed in magnetic field as the position of the conductor changes from center to I_4 position.

4 Testing of RC model

Section 4 discusses the testing of RC model by supplying two different input signals. Sinusoidal high magnitude

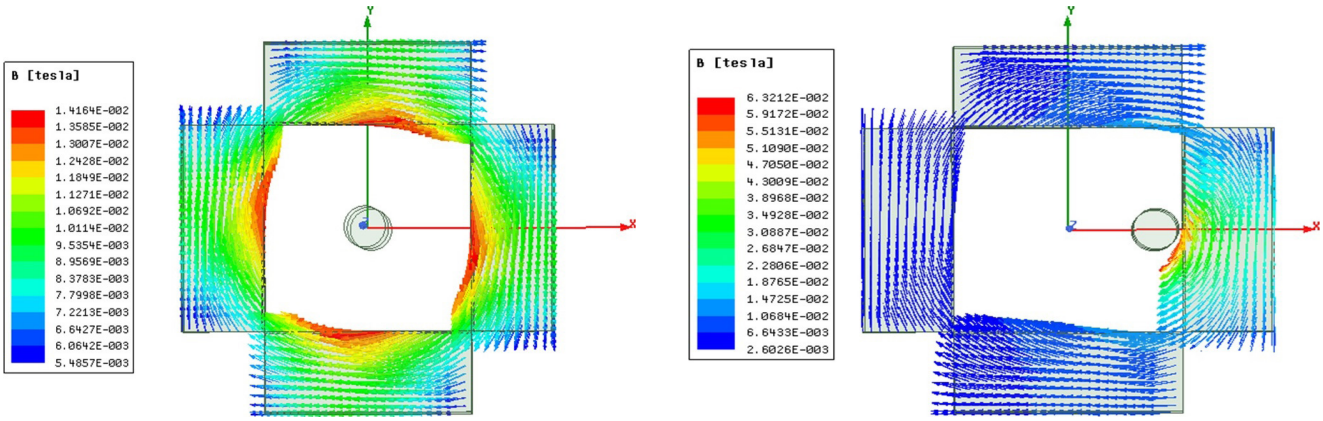

(a) (b)

Fig. 10 Magnetic field distribution for RC model with S = 4: (a) conductor placed at center; (b) conductor placed at I_4 position

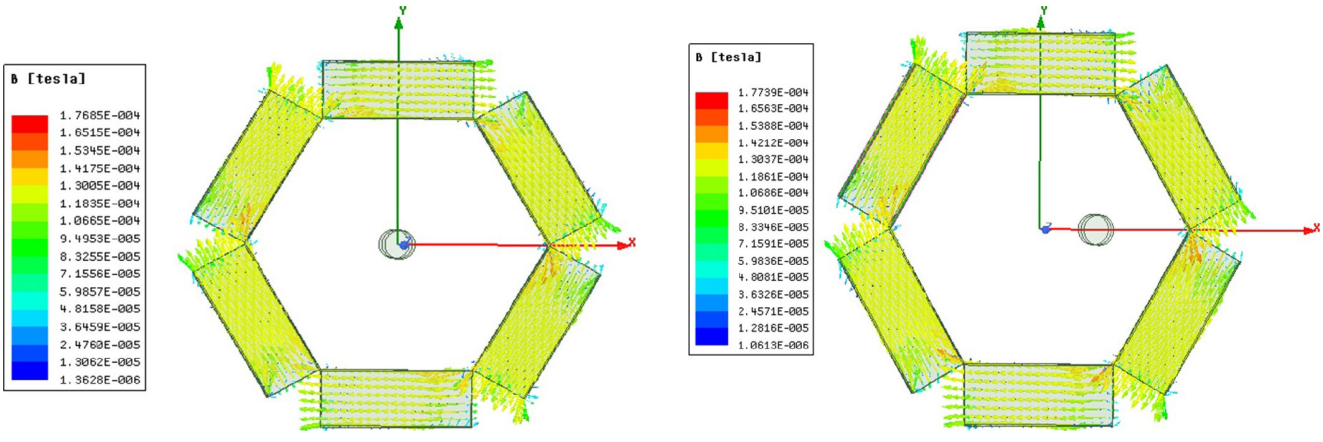

(a) (b)

Fig. 11 Magnetic field distribution for RC model with S = 6: (a) conductor placed at center; (b) conductor placed at I_4 position

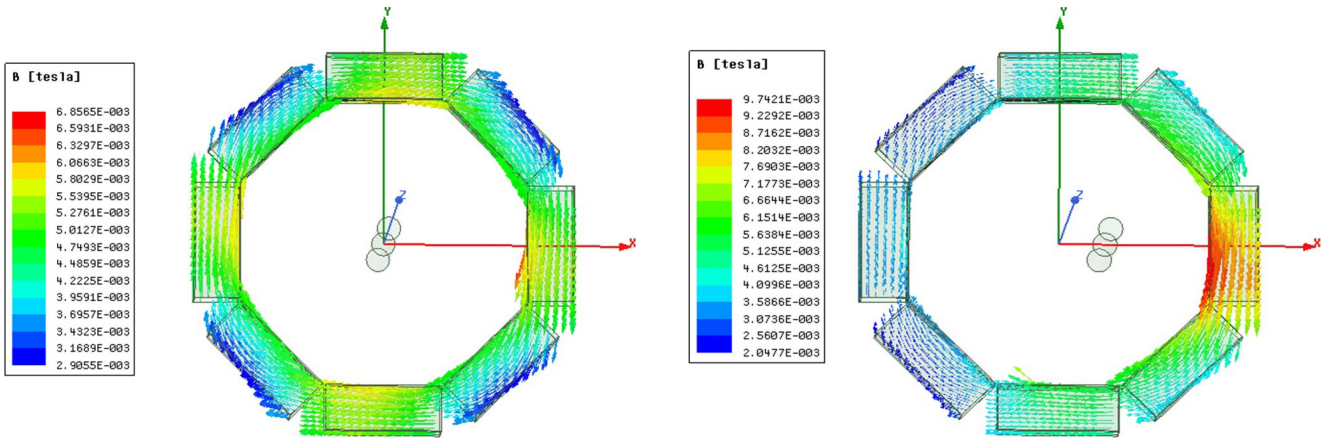

(a) (b)

Fig. 12 Magnetic field distribution for RC model with: $S = 8$: (a) conductor placed at center; (b) conductor placed at I_4 position

power frequency and high magnitude impulse current are applied as an input to a RC model. For simulation purpose four rectilinear S ($S = 4$) and circular cross-section of primary conductor with radius of 1 mm are considered. The number of turns considered for RC_1 and RC_3, is 500. Similarly, for RC_2 and RC_4, the number of turns is 1000. The length of S considered is $L_1 = 10$ mm and $L_2 = 20$ mm as illustrated in Fig. 3.

4.1 Sinusoidal power frequency current as an input to primary conductor

The circuit for testing of RC model, by applying an input sinusoidal current having high amplitude low frequency is illustrated in Fig. 13. The input given to the conductor is varied from 50 to 500 A with the frequency of 50 Hz. In the circuit, R_1 and R_2 are taken as 1 Ω and 10 Ω, respectively. S RC_1, RC_2, RC_3 and RC_4 shown in Fig. 13 are represented Winding1, Winding2, Winding3 and Winding4, respectively and they are connected in series. The induced voltage of a coil is measured between the input terminal of Winding1 and the output terminal of Winding4.

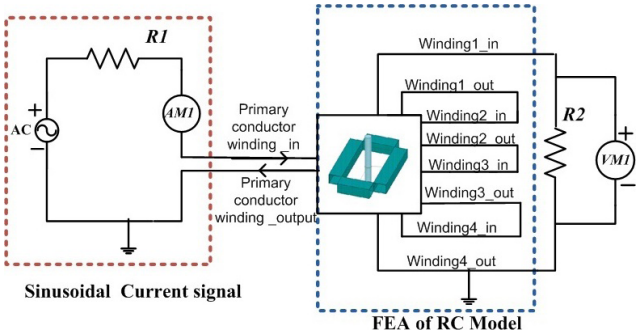

Fig. 13 Circuit for testing RC model with sinusoidal power frequency signal

The induced output voltage obtained for the designed RC model is shown in Fig. 14. For a 400 A root mean square (RMS) input, 115.1565 mV induced voltage is obtained. As the RC model output voltage leads primary current by 90°. In order to calculate the RC model sensitivity, the coil is tested for a different input current as reported in Table 3.

The input current is varied from 50 to 500 A (RMS), produces the corresponding output voltage from 14.44 to

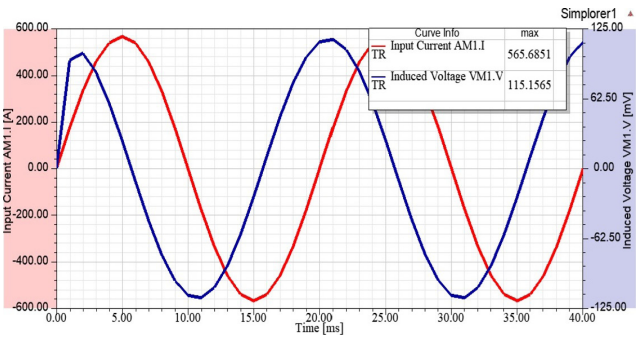

Fig. 14 Simulation result of the induced voltage of RC model across R_2 for input current of 400 A (RMS) from ANSYS Maxwell [28] environment

Table 3 Sinusoidal input current and induced output voltage of RC model

S. No.	Input current (RMS) (A)	Input current (max) (A)	Induced voltage (max) (mV)	Sensitivity (mV/A)
1	50	70.71	14.3946	0.203572
2	100	141.42	28.7892	0.203572
3	150	212.13	43.1837	0.203571
4	200	282.84	57.5783	0.203571
5	250	353.55	71.9728	0.203571
6	300	424.26	86.3677	0.203572
7	350	494.97	100.7620	0.203571
8	400	565.68	115.1565	0.203571
9	450	636.39	129.5513	0.203572
10	500	707.10	143.9455	0.203571

143.945 mV. The sensitivity observed for the RC model is ≈ 0.2035 mV/A. To enhance clarity, the graph is plotted between input current and induced voltage (RC output voltage) and shown in Fig. 15. Fig. 15 illustrates that the output induces voltage is, follows linear with the supply, and the RC does not enter the saturation region. The sensitivity of coil is nearly same for the given range of testing input signal.

4.2 Impulse current as an input to primary conductor

Testing with impulse currents that have a high magnitude is an important component for RC model. Section 4.2 discusses the testing of RC model by supplying 8/20 μs impulse current and it is shown in Fig. 16. The Fig. 16 consists of two parts that is impulse current generator circuit and Finite Element Analysis (FEA) of RC model. The RC primary current (input current) is produced by impulse current generator circuit, that involve of DC charging voltage (VDC), current limiting resistor (R_3), wave shaping resistor inductor and capacitor (R, L and C).

The RLC transient circuit produces 8/20 μs impulse current i_m [31]. Through DC supply capacitor is charged to a certain value and discharged through the wave shaping resistor and inductor. The generated impulse current i_m [31] is expressed in Eq. (4) and the same is supplied to primary conductor to test the RC model:

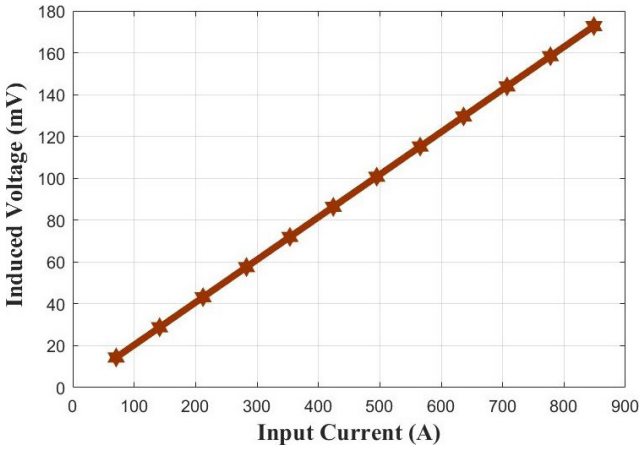

Fig. 15 Induced voltage of RC model as a function of sinusoidal testing input current

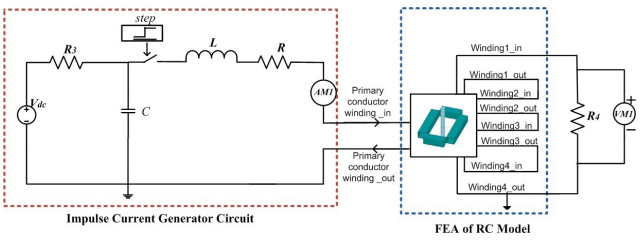

Fig. 16 Circuit for testing RC model with 8/20 μs impulse current signal

$$i_m = \frac{V}{\omega L} e^{-\alpha t} \sin(\omega t), \tag{4}$$

where V is capacitor charging voltage:

$$\alpha = \frac{R}{2L}, \tag{5}$$

$$\omega = \sqrt{\frac{1}{LC} - \frac{R_2}{4L_2}}, \tag{6}$$

As per IS/IEC 60060-2 (2010) standard [32], the time required for the current to increase from zero to the initial peak value can be determined using Eq. (7) and the time taken for half value of peak in the tail portion time is calculated using Eq. (8):

$$\text{Front time } (T_1) = \frac{1}{\omega} \sin^{-1}\left(\frac{\omega}{\sqrt{LC}}\right), \tag{7}$$

$$\text{Tail time } (T_2) = \frac{\pi}{\sqrt{\left(\frac{1}{LC}\right) - \left(\frac{R_2}{4L_2}\right)}}. \tag{8}$$

For 8/20 μs impulse current, the aforementioned value is used [33]:

$$\alpha = 0.0535 \times 10^6 \text{ and } \omega = 0.113 \times 10^6,$$

$$LC = 65, \tag{9}$$

$$i_m = \frac{VC}{14}. \tag{10}$$

For simulation purpose, consider energy storage capacitor, wave shaping inductor and resistor are 0.6 μF, 110 μH and 12 Ω, respectively. The value of current limiting resistor (R_3) and load resistor (R_4) are chosen to 200 kΩ and 10 Ω, respectively. The testing of RC model with high magnitude high frequency impulse current (8/20 μs) for different DC charging voltage are given in Table 4. From simulation result ammeter AM1 and voltmeter VM1 shows the impulse current (input current) and induced voltage (output of RC) waveform. RC model induced voltage 1.2906 V is observed for impulse current input peak of 396.19 A with the charging voltage of 10 kV is illustrated in Fig. 17. The sensitivity of coil is 3.2574 mV/A. The front time (T_1) and tail time (T_2) of the induced voltage is matched with input current, which are 7 μs and 20.2 μs, respectively.

According to IEC standard, this front time and tail time are adequate. In order to calculate the RC model sensitivity, the coil is tested for a different input current

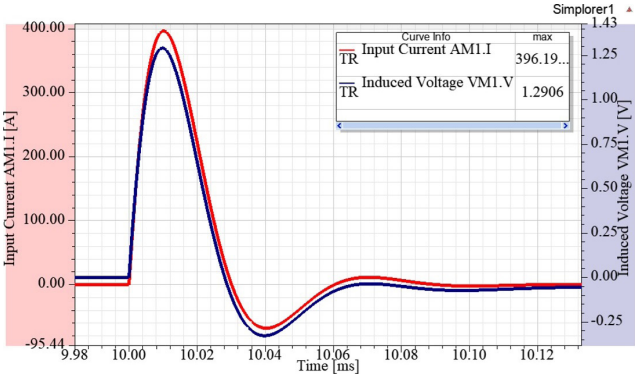

Fig. 17 Simulation result of induced voltage of RC model for input impulse (8/20 µs) current with peak of 396.19 A from ANSYS Maxwell [28] environment

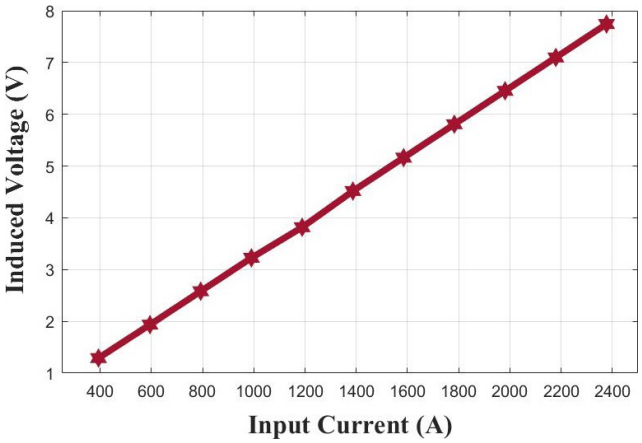

Fig. 18 Induced voltage of RC model as a function of impulse (8/20 µs) testing input current

as reported in Table 4. The input current is varied from 396.19 to 2179.09 A. the corresponding charging voltage range is 10 to 55 kV. The output induced voltage observed is 1.2906 to 7.0981 V with sensitivity ≈ 3.2574 mV/A. Those data are reported in Table 4. The graph is plotted between input impulse current and RC model output and shown in Fig. 18. From Fig. 18, it is seen that voltage waveforms are not distorted, follow linear patterns.

5 Conclusion and future work

This paper presents a discrete RC model composed of rectilinear *S* connected in series. The *M* between the RC model and the primary conductor was computed using the FEM. The effect of different primary conductor cross-sections, including circular, rectangular, and D-shaped, on *M* has been analyzed concerning the conductor's position. *M* is nearly equal for centrally placed circular and rectangular conductors, while off-center positioning increases it for nearby *S*. The FEM results show that the E is 2.229% for circular, 0.024822% for rectangular, and 0.5533% for D-shaped conductors. The influence of the eccentricity of the conductor considering the number of *S* is examined. This study observes a maximum *E* of 3% for RC models with $S = 8$. The results indicate that *E* decreases as the number of *S* increases. The magnetic field distribution varies with conductor position, with a maximum of 5.486×10^{-3} *T* observed for $S = 4$. The sensitivity of the designed RC with $S = 4$ is tested with different magnitude of power and high frequency impulse (8/20 µs) current signals. The simulation results show consistent output characteristics, with observed sensitivities of 0.2035 mV/A for sinusoidal current and 3.257 mV/A for impulse current.

Table 4 Impulse input current and output induced voltage of RC model

S. No.	DC voltage (kV)	Input current (max) (A)	Induced voltage (max) (V)	Sensitivity (mV/A)
1	10	396.19	1.2906	3.25747
2	15	594.29	1.9358	3.25733
3	20	792.39	2.5811	3.25736
4	25	990.49	3.2264	3.25735
5	30	1188.59	3.8717	3.25738
6	35	1386.69	4.5170	3.25739
7	40	1584.79	5.1622	3.25739
8	45	1782.89	5.8075	3.25735
9	50	1980.99	6.428	3.25736
10	55	2179.09	7.0981	3.25736

This study provides a detailed analysis of a discrete RC model; however, further research is necessary to enhance its accuracy and practical applicability. Future work includes the experimental validation of simulation results by fabricating and testing a physical RC prototype. Additionally, a detailed investigation is required to assess the impact of higher-frequency transient currents on RC performance. Exploring alternative S materials with lower resistivity and improved thermal stability can help minimize losses and improve efficiency.

Acknowledgement

The authors would like to thank the respected reviewers for their valuable suggestions to improve the quality of the manuscript.

References

[1] Ramboz, J. D. "Machinable Rogowski coil, design, and calibration", IEEE Transactions on Instrumentation and Measurement, 45(2), pp. 511–515, 1996. https://doi.org/10.1109/19.492777

[2] Samimi, M. H., Mahari, A., Farahnakian, M. A., Mohseni, H. "The Rogowski Coil Principles and Applications: A Review", IEEE Sensors Journal, 15(2), pp. 651–658, 2015. https://doi.org/10.1109/JSEN.2014.2362940

[3] Han, S., Han, X., Sun, W. "The Analysis of Magntic Flux Density Inside Rogowski Coil Based on Full Current Theory", IEEE Sensors Letters, 4(7), 2500704, 2020. https://doi.org/10.1109/LSENS.2020.2987707

[4] Xu, M., Yan, J., Geng, Y., Zhang, K., Sun, C. "Research on the Factors Influencing the Measurement Errors of the Discrete Rogowski Coil", Sensors, 18(3), 847, 2018. https://doi.org/10.3390/s18030847

[5] Sun, C., Yan, J., Geng, Y., Zhang, K., Xu, M., Liu, J. "Research on a novel current transducer based on discrete Rogowski coils", In: 2016 International Conference on Condition Monitoring and Diagnosis (CMD), Xi'an, China, 2016, pp. 798–801. ISBN 978-1-5090-3399-7 https://doi.org/10.1109/CMD.2016.7757947

[6] Dongwei, L., Di Rienzo, L. "Modeling arrays of rectilinear solenoids for current sensing", In: 2011 1st International Conference on Electric Power Equipment - Switching Technology, Xi'an, China, 2011, pp. 674–677. ISBN 978-1-4577-1273-9 https://doi.org/10.1109/ICEPE-ST.2011.6122909

[7] Mingotti, A., Betti, C., Tinarelli, R., Peretto, L. "Simplifying Rogowski Coil Modeling: Simulation and Experimental Verification", Sensors, 23(19), 8032, 2023. https://doi.org/10.3390/s23198032

[8] Liu, X., Huang, H., Jiao, C. "Modeling and Analyzing the Mutual Inductance of Rogowski Coils of Arbitrary Skeleton", Sensors, 19(15), 3397, 2019. https://doi.org/10.3390/s19153397

[9] Liu, X., Huang, H., Cui, Y., Dai, Y., Liu, X. "Mutual Inductance Between Arbitrary Conductor and Rogowski Coil With Circular Skeleton and Gap Compensation", IEEE Sensors Journal, 19(11), pp. 4106–4114, 2019. https://doi.org/10.1109/JSEN.2019.2896443

[10] Marracci, M., Tellini, B., Zappacosta, C., Robles, G. "Critical Parameters for Mutual Inductance Between Rogowski Coil and Primary Conductor", IEEE Transactions on Instrumentation and Measurement, 60(2), pp. 625–632, 2011. https://doi.org/10.1109/TIM.2010.2051591

[11] Ferković, L., Ilić, D., Malarić, R. "Mutual Inductance of a Precise Rogowski Coil of the Position of Primary Conductor", IEEE Transactions on Instrumentation and Measurement, 58(1), pp. 122–128, 2009. https://doi.org/10.1109/TIM.2008.928412

[12] Ferković, L., Ilić, D., Leniček, I. "Influence of Axial Inclination of the Primary Conductor on Mutual Inductance of a Precise Rogowski Coil", IEEE Transactions on Instrumentation and Measurement, 64(11), pp. 3045–3054, 2015. https://doi.org/10.1109/TIM.2015.2444254

[13] Chen, Q., Li, H., Zhang, M., Liu, Y. "Design and Characteristics of Two Rogowski Coils Based on Printed Circuit Board", IEEE Transactions on Instrumentation and Measurement, 55(3), pp. 939–943, 2006. https://doi.org/10.1109/TIM.2006.873788

[14] Wang, J., Chen, W., Chen, P. "A Design Method of PCB Rogowski Coil in Limited Space and Modified Integral Circuit", IEEE Sensors Journal, 20(11), pp. 5801–5808, 2020. https://doi.org/10.1109/JSEN.2020.2974403

[15] Liu, Y., Xie, X., Hu, Y., Qian, Y., Sheng, G., Jiang, X. "A Novel Transient Fault Current Sensor Based on the PCB Rogowski Coil for Overhead Transmission Lines", Sensors, 16(5), 742, 2016. https://doi.org/10.3390/s16050742

[16] Xu, Y., Zou, X., Wang, X. "Influencing Factors and Error Analysis of Pulse Current Measurement With Air-Core Rogowski Coil", IEEE Transactions on Plasma Science, 48(12), pp. 4381–4386, 2020. https://doi.org/10.1109/TPS.2020.3030691

[17] Halim, N. H., Azmi, A., Yahya, Y., Abdullah, F., Othman, M., Laili, M. S. "Development of a small scale standard lightning impulse current generator", In: 2011 5th International Power Engineering and Optimization Conference, Shah Alam, Malaysia, 2011, pp. 426–431. ISBN 978-1-4577-0355-3 https://doi.org/10.1109/PEOCO.2011.5970422

[18] Istrate, D., Blanc, I., Fortuné, D. "Development of a Measurement Setup for High Impulse Currents", IEEE Transactions on Instrumentation and Measurement, 62(6), pp. 1473–1478, 2013. https://doi.org/10.1109/TIM.2013.2239018

[19] Metwally, I. A. "Self-Integrating Rogowski Coil for High-Impulse Current Measurement", IEEE Transactions on Instrumentation and Measurement, 59(2), pp. 353–360, 2010. https://doi.org/10.1109/TIM.2009.2023821

[20] Metwally, I. A. "Performance Improvement of Slow-Wave Rogowski Coils for High Impulse Current Measurement", IEEE Sensors Journal, 13(2), pp. 538–547, 2013. https://doi.org/10.1109/JSEN.2012.2222372

[21] Argüeso, M., Robles, G., Sanz, J. "Measurement of high frequency currents with a Rogowski coil", Congreso Hispano-Luso de Ingenieria Eléctrica, 76(6), pp. 65101–65107, 2005.

[22] Dubickas, V., Edin, H. "High-Frequency Model of the Rogowski Coil With a Small Number of Turns", IEEE Transactions on Instrumentation and Measurement, 56(6), pp. 2284–2288, 2007. https://doi.org/10.1109/TIM.2007.907965

[23] Patel, T. P., Vora, S. C. "FE based eccentricity analysis of Rogowski Coil", In: 2016 IEEE 1st International Conference on Power Electronics, Intelligent Control and Energy Systems (ICPEICES), Delhi, India, 2016, pp. 1–6. ISBN 978-1-4673-8588-6 https://doi.org/10.1109/ICPEICES.2016.7853568

[24] Marracci, M., Tellini, B., Zappacosta, C. "FEM Analysis of Rogowski Coils Coupled with Bar Conductors", In: 19th IMEKO World Congress, Lisbon, Portugal, 2009, pp. 887–891. ISBN 978-963-88410-0-1

[25] Draxler, K., Styblíková, R. "Magnetic Shielding of Rogowski Coils", IEEE Transactions on Instrumentation and Measurement, 67(5), pp. 1207–1213, 2018. https://doi.org/10.1109/TIM.2018.2810618

[26] Ayhan, B., Uçak, C. "Improved Magnetic Circuit Model for Magnetic Shielding Effectiveness in Rogowski Coil", IEEE Transactions on Magnetics, 56(3), 8500109, 2020. https://doi.org/10.1109/TMAG.2019.2958534

[27] Fu, S., Deng, E., Peng, C., Zhang, G., Zhao, Z., Cui, X. "Method of Turns Arrangement of Noncircular Rogowski Coil With Rectangular Section", IEEE Transactions of Instrumentation and Measurement, 70, 9000310, 2021. https://doi.org/10.1109/TIM.2020.3024507

[28] ANSYS, Inc. "ANSYS Maxwell 2D/3D Field Simulator, (R1 version 2022)", [online] Available at: https://www.ansys.com/products/electronics/ansys-maxwell [Accessed: 05 June 2023]

[29] Bawankule, P., Chandrasekaran, K. "Modeling and Design of Rogowski Coil for Pulsed Current Signal Measurement With Analytical, Experimental, and Finite Element Method", IEEE Transactions on Plasma Science, 52(7), pp. 2965–2974, 2024. https://doi.org/10.1109/TPS.2024.3424935

[30] Bawankule, P., Chandrasekaran, K. "Modeling and Designing of Rogowski Coil for High-Frequency Sinusoidal Signal Measurement with Finite Element and Experimental Method", Arabian Journal for Science and Engineering, 50(8), pp. 5559–5571, 2025. https://doi.org/10.1007/s13369-024-09410-x

[31] Bawankule, P., Chandrasekaran, K. "Rogowski Coil with an Active Integrator for Impulse Current Measurement", In: 2022 IEEE 3rd Global Conference for Advancement in Technology (GCAT), Bangalore, India, 2022, pp. 1–5. ISBN 978-1-6654-6856-5 https://doi.org/10.1109/GCAT55367.2022.9971975

[32] BIS "IS/IEC 60060-2 (2010) High – Voltage Test Techniques, Part 2: Measuring Systems", Bureau of Indian Standards, New Delhi, India, 2010. [online] Available at: https://law.resource.org/pub/in/bis/S05/is.iec.60060.2.2010.pdf [Accessed: 25 May 2025]

[33] Naidu, M. S., Kamaraju, V. "High-Voltage Engineering", McGraw Hill Education, 2009. ISBN 978-1-25-906289-6